Research Article | Vol. 28, No. 18 / 31 August 2020 / Optics Express 27037
Optics EXPRESS

Space-division multiplexed transmission in the S-band over 55 km few-mode fibers

GEORG RADEMACHER,[1,*] BENJAMIN J. PUTTNAM,[1] RUBEN S. LUIS,[1] LIDIA GALDINO,[2] RYO MARUYAMA,[3] KAZUHIKO AIKAWA,[3] YOSHINARI AWAJI,[1] AND HIDEAKI FURUKAWA[1]

[1]National Institute of Information and Communications Technology, Photonic Network System Laboratory, 4-2-1, Nukui-Kitamachi, Koganei, Tokyo 184-8795, Japan
[2]Optical Networks Group, University College London, Torrington Place, London WC1E 7JE, UK
[3]Fujikura Ltd, 1440, Mutsuzaki, Sakura, Chiba 285-8550, Japan
[*]georg.rademacher@nict.go.jp

Abstract: Transmission of highly spectral efficient 24.5 GBaud quadrature phase shift keying and 16- and 64-quadrature amplitude modulated signals in the S-band between 1492 nm and 1518 nm wavelength is demonstrated over 55 km few-mode fibers. The carrier lines for S-band transmission were generated by a single wideband optical comb source with more than 120 nm optical bandwidth. While the three-mode fiber was originally optimized for C- and L-band transmission, we show that differential mode delay and mode-dependent loss show only a minor wavelength dependence within the measured S-band channels. However, the transceiver sub-system, including S-band optical amplifiers as well as a reduced optical signal-to-noise ratio of the comb source, leads to a significant Q-factor penalty for channels towards the edges of the S-band optical amplifiers below 1495 nm and above 1515 nm wavelength.

1. Introduction

Space-division multiplexing (SDM) is an attractive technique to increase the per-fiber data-rates in optical transmission systems by transmitting independent data channels at the same wavelength over different spatial channels [1]. Various fiber types have been reported for using SDM, including coupled- and un-coupled multi-core fibers (MCF) [2,3], few- and multi-mode fibers (FMF, MMF) [4,5] as well as few-mode multi-core fibers (FM-MCF) with up to 120 spatial channels [6] and a maximum per-fiber data rate of 10.66 Pb/s [7].

At the same time, ultra wideband wavelength-division multiplexed (WDM) or multi-band transmission beyond the C-band is discussed as an option to increase the data rates in standard single-mode fibers (SMF) [8–10]. A recent study combined uncoupled MCF with S-,C-, and L-band transmission, showing great potential of combining SDM with multi-band transmission for a total data rate of 0.61 Pb/s in a 125 micro-meter cladding diameter 4-core MCF [11].

In this work, we demonstrate transmission of quadrature phase shift keying (QPSK), 16-, and 64-quadrature amplitude modulated (QAM) signals over 55 km three-mode fiber. To generate signals in the S-band, carrier lines are produced by a single optical comb source with more than 120 nm bandwidth. We analyze the wavelength dependence of mode-dependent loss and the delay-spread of the fiber's impulse response. Being the first demonstration of S-band transmission in FMF, this study indicates no significant performance penalty resulting from transmission, while several components of the transceiver subsystems show a penalty compared to previous transmission experiments in C- and L-bands.

#399791 https://doi.org/10.1364/OE.399791
Journal © 2020 Received 8 Jul 2020; revised 19 Aug 2020; accepted 19 Aug 2020; published 28 Aug 2020

Optics EXPRESS

2. Experimental setup

The experimental setup used to investigate S-band transmission over FMF is shown in Fig. 1. A single optical comb source, based on a 5 kHz linewidth seed laser, generated more than 600 carrier lines in a 25 GHz grid, with an OSNR of up to 45 dB in the center of the comb at approximately 1559 nm wavelength. A tunable optical bandpass filter selected a single carrier line that was amplified in a semiconductor optical amplifier (SOA) before modulation in a dual-polarization IQ-modulator (DP-IQ). The DP-IQ modulator was driven by a four channel arbitrary waveform generator (AWG), operating at 49 GSample/s and generating 24.5 GBaud root-raised cosine shaped QPSK, 16- or 64-QAM signals with a roll-off factor of 0.01. The signal was amplified in a Thulium doped fiber amplifier (TDFA) with a total output power of 20 dBm and noise figure of around 5 dB [12].

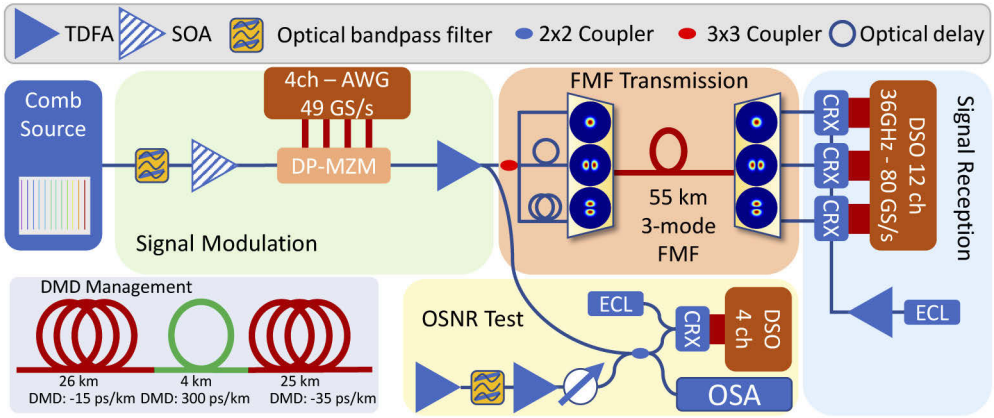

Fig. 1. Experimental setup for demonstration of few-mode fiber transmission in the S-band with a single optical comb source as light source.

The signal was split in a 1x3 splitter with two arms delayed by approximately 94 ns and 193 ns (20m and 40m optical patchcord), emulating independent data patterns on the three paths that formed a spatial super channel (SSC), while preserving the coherence of the transmitted signal. The three signals were coupled in and out of the FMF through a laser-inscriped 3-D waveguide mode-selected multiplexer with approximately 1.5 dB insertion loss and mode selectivity of more than 16 dB [13]. The FMF link supported the two-fold degenerate LP_{01} mode group and the four-fold degenerate LP_{11} mode group for a total of three spatial modes [14]. The link was differential mode-delay (DMD) compensated, as shown in the inset in Fig. 1, and consisted of three spools of graded-index three mode fiber with DMDs of -15 ps/km, +300 ps/km and -35 ps/km, with lengths of 26 km, 4 km and 25 km, respectively, at 1550 nm wavelength for a nominal delay of around 100 ps between modes. All fiber modes had a chromatic dispersion of approximately 20 ps/nm/km at 1550 nm wavelength. The fiber had a loss of 0.20 dB/km at 1550 nm wavelength for a total link loss of approximately 14 dB including both multiplexers. The launch power per channel / mode was approximately 8 dBm.

The three signals were received in three coherent receivers, where the signals were mixed with a local oscillator with less than 100 kHz linewidth. The electrical signals were digitized in a 12-channel real time oscilloscope (DSO) at 80 GSample/s with an electrical bandwidth of 36 GHz. Offline digital signal processing (DSP) consisted of a 6×6 time-domain multiple-input / multiple-output (MIMO) equalizer that was initialized in a data-aided mode before switching to a decision-directed mode after equalizer convergence. A phase-recovery algorithm was running within the equalizer loop [15]. Q-Factors were calculated from the bit-error-rate (BER) that was

Optics EXPRESS

estimated from more than 2 million symbols per measurement. We further calculated the data rate per wavelength channel based on generalized mutual information (GMI), assuming ideal codes and bit-wise decoding. To characterize the transceiver sub-system, an optical signal to noise (OSNR) test was performed according to the setup in the lower section of Fig. 1. The signal after modulation was combined with amplified spontaneous emission (ASE) noise, generated by a two stage TDFA with a filter in between to increase the noise power spectral density. The OSNR was controlled by setting the noise power in a variable optical attenuator (VOA) and measured in an optical spectrum analyzer (OSA).

3. Transceiver characterization

To characterize the back-to-back performance of the transceiver sub-system with QPSK, 16- and 64-QAM signals, OSNR scans were performed for wavelength channels, between 1492 nm and 1514 nm wavelength. Figure 2 shows the Q-factors as a function of the OSNR for four wavelength channels and the three analyzed modulation formats together with the theoretical performance in an additive white Gaussian noise channel, as reference. For QPSK and at low Q-Factors, all wavelength channels have a similar implementation penalty compared to the theoretical line of approximately 0.5 dB OSNR, increasing to about 1 dB at a Q-Factor of 12 dB. For 16-QAM and at low Q-Factors, the implementation penalty is less than 1 dB, increasing to several dB for Q-Factors above 8 dB. The wavelength channel at 1492 nm wavelength has significantly decreased performance compared to the three other wavelength channels. For 64-QAM signals a strong implementation penalty of more than 4 dB at a Q-Factor of 5 dB can be observed that increases for higher Q-Factors with a strong wavelength dependence. The implementation penalty compared to previous measurements in the C-Band is approximately 3 dB larger [16].

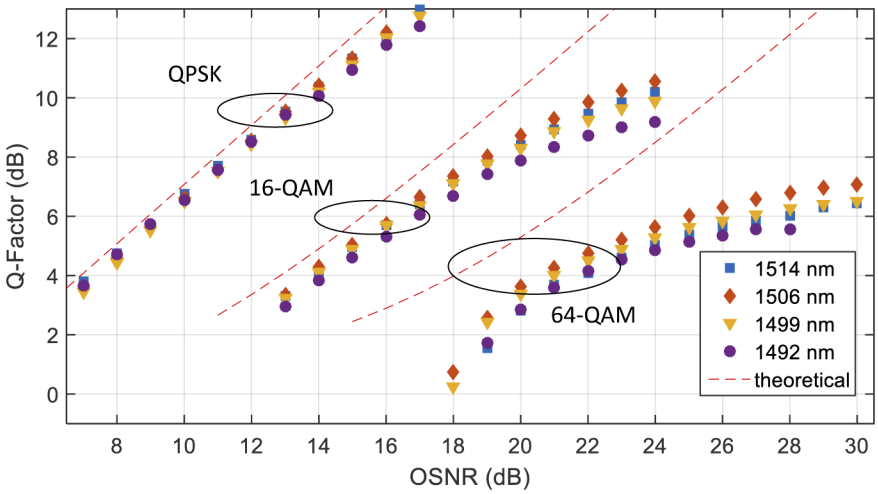

Fig. 2. Q-Factor as a function of the optical signal to noise ratio (OSNR), evaluated in 0.1 nm bandwidth, for dual-polarization (DP-) (a) QPSK, (b) 16-QAM and (c) 64-QAM signals for four different wavelength channels. Theoretical performance in an additive white Gaussian noise (AWGB) channel model as reference.

We further calculated the required OSNR (ROSNR) at an arbitrarily chosen BER threshold of 3×10^{-2}, corresponding to a Q-Factor of approximately 5.5 dB, for the three modulation formats and wavelength channels between 1492 nm and 1514 nm, as shown in Fig. 3. While QPSK has no visible wavelength dependence, 16-QAM has shows a mild increase of approximately 1 dB towards to lower band edge. 64-QAM has the strongest wavelength dependence, visible on both

Optics EXPRESS

band edges, with a minimum ROSNR of 23.4 dB at 1508 nm wavelength, increasing to 26.6 dB at 1492 nm and 25.3 dB at 1514 nm wavelength.

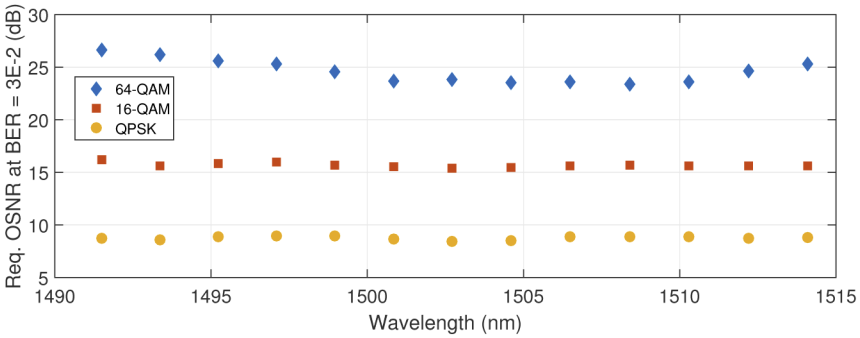

Fig. 3. Q-Factor as a function of the optical signal to noise ratio (OSNR), evaluated in 0.1 nm bandwidth, for dual-polarization (DP-) (a) QPSK, (b) 16-QAM and (c) 64-QAM signals for four different wavelength channels. Theoretical performance in an additive white Gaussian noise (AWGB) channel model as reference.

We attribute the Q-Factor penalty at the band edges to three effects: at the band edges of the S-Band, the used TDFA has suboptimal gain and a slightly increased noise figure, as reported in [12]. Furthermore, the OSNR of the comb source degrades towards the lower measured wavelength channels [11]. Finally, transceiver components, such as the IQ-modulator, receiver hybrid and balanced photo diodes were optimized for C- (and L-) band operation.

4. Transmission channel characterization

Loss and DMD of the three-mode FMF transmission link were optimized for C- and L-band transmission [14]. To demonstrate its compatibility with S-band transmission, we analyzed the delay spread and mode-dependent loss (MDL) for various wavelength channels. Delay spread and MDL were calculated from the channel matrix that was estimated by running the MIMO equalizer in the reversed direction as detailed in [17], using QPSK modulated data.

Figure 4(a) shows the impulse response of three wavelength channels. Two distinct time intervals with significant contributions to the impulse response represent the accumulated delay spread of the two mode groups. It further indicates a low level of distributed coupling during

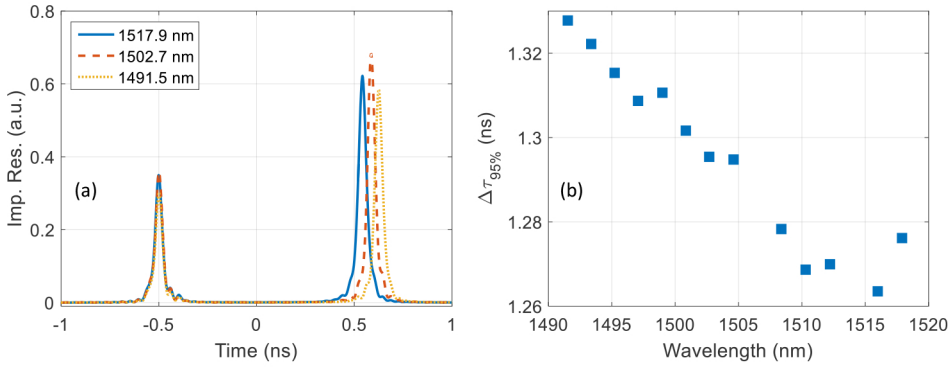

Fig. 4. (a) Impulse response of three wavelength channels. (b) Impulse response spread, represented by the time span that covers 95% of the contributions of the impulse response.

Optics EXPRESS

transmission that would lead to a plateau in between the two peaks. Figure 4(b) shows the wavelength dependence of the impulse response duration, here defined as the time spread that covers 95% of the contributions to the impulse response. The impulse response increases almost linearly with decreasing wavelength, as expected for a fiber that is DMD optimized for C- and L-band transmission. Nevertheless, the impulse response length increase is less than 70 ps in total, or 1.3 ps/km over a wavelength range of more than 25 nm.

Figure 5(a) shows the frequency distribution of the squared singular values of the 6×6 channel matrix. No significant fluctuations can be observed with frequency, compared to e.g. long haul transmission in the C-band, as reported in [17]. Figure 5(b) shows the MDL, calculated as the ratio between maximum and minimum of the frequency-averaged squared singular values, for all measured wavelength channels. For all but one channel, MDL is below 2.1 dB, while a trend of increasing MDL can be observed for decreasing wavelengths. The wavelength channel at 1491.5 nm wavelength has MDL above 3 dB, presumably due to low signal quality, impairing the MDL estimation. The reported MDL values are in agreement with previously reported values for C- and L-band transmission [4], hence indicating little or no additional penalty from transmitting in the S-band.

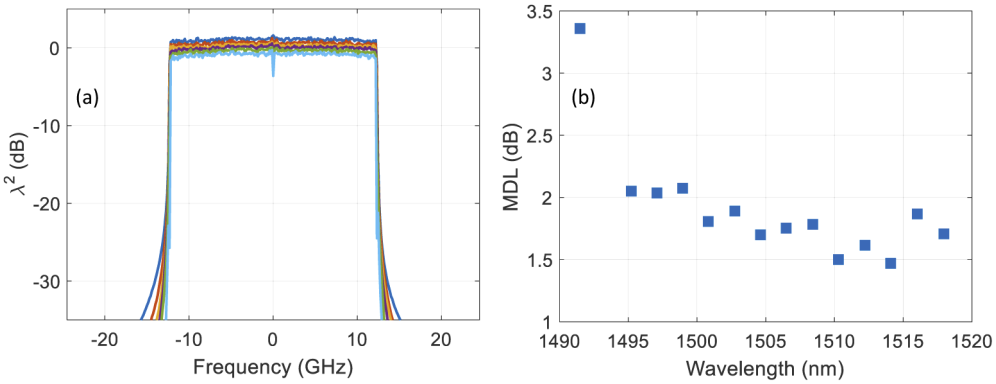

Fig. 5. (a) Spectral dependence of the singular values of the six tributaries of the channel matrix. (b) Mode-dependent loss (MDL) of all measured wavelength channels.

5. Transmission results

Figure 6(a) shows the Q-Factors of all measured wavelength channels. Every 10 channels were measured within the 25 GHz channel grid. For most QPSK channels, no errors were detected, here marked as a Q-Factors of 15 dB. Figure 6(b) shows the data rate for each measured wavelength channel, estimated from GMI. We note that for some channels, the 10-channel measurement grid couldn't strictly be followed as the local oscillator laser had technical issues stabilizing at certain wavelengths. In such case, the neighbor channel was measured.

For QPSK, the performance is almost flat across all wavelength channels, only the wavelength channel at 1492 nm had a significantly reduced Q-Factor. Data rates were around 280 Gb/s per wavelength channel. For 16-QAM signals, Q-Factors varied between 4 and 11 dB, peaking at 1510 nm wavelength and reducing towards both edges of the bands. Data rates per channel ranged from 450 Gb/s to almost 600 Gb/s. For 64-QAM signals, Q-Factors were between -0.5 dB and 6 dB with data rates between 380 Gb/s and 800 Gb/s.

The measured transmission performance after 55 km three-mode fiber was consistent with the transmitter characteristics as reported in section 3.. As the transmission channel characteristics, especially MDL, were shown to be only mildly wavelength dependent, we conclude that the wavelength dependent performance is dominated by the transceiver sub-system, including S-band

Optics EXPRESS

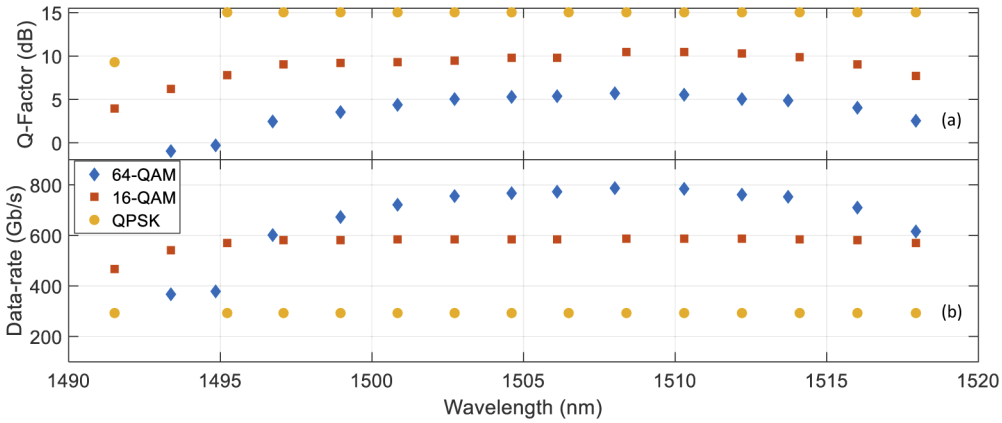

Fig. 6. (a) Q-Factors and (b) data rates, calculated from generalized mutual information for every 10 wavelength channels between 1492 nm and 1518 nm wavelength with QPSK, 16- and 64-QAM modulation.

optical amplifiers. Consequently, combining FMFs with multi-band transmission, including the S-band is a promising technology to increase the per-fiber capacity beyond transmitting spatially-multiplexed data in the C-band.

6. Conclusion

We have reported space-division multiplexed transmission in the S-band over 55 km few-mode fiber with wavelength channels between 1491.5 nm and 1517.9 nm. We have shown that the impulse response spread increases weakly towards lower wavelengths, with a total delay spread increase of less than 70 ps over the wavelength span of more than 25 nm. We further analyzed mode-dependent loss, showing a moderate increase towards lower wavelength channels with values below 2.1 dB for all but one channel. We have further reported transmission of 24.5 GBaud quadrature-phase shift keying as well as 16- and 64-quadrature amplitude modulated signals. We found that the transmission performance is mostly impacted by transceiver and optical amplifier noise. We have reported data rates of up to 800 Gb/s per wavelength channel, demonstrating the feasibility of combining few-mode fibers with S-band transmission.

Funding

Royal Society; Royal Academy of Engineering; Engineering and Physical Sciences Research Council (TRANSNET EP/R035342/1).

Disclosures

The authors declare no conflicts of interest.

References

1. D. Richardson, J. Fini, and L. Nelson, "Space-division multiplexing in optical fibres," Nat. Photonics **7**(5), 354–362 (2013).
2. G. Rademacher, R. S. Luís, B. J. Puttnam, R. Ryf, S. van der Heide, T. A. Eriksson, N. K. Fontaine, H. Chen, R.-J. Essiambre, Y. Awaji, H. Furukawa, and N. Wada, "172 Tb/s C+L Band Transmission over 2040 km Strongly Coupled 3-Core Fiber," in *Optical Fiber Communication Conference Postdeadline Papers 2020* (Optical Society of America, 2020), pp. Th4C.5.

Optics EXPRESS

3. B. Puttnam, R. Luís, E. Agrell, G. Rademacher, J. Sakaguchi, W. Klaus, G. Saridis, Y. Awaji, and N. Wada, "High capacity transmission systems using homogeneous multi-core fibers," J. Lightwave Technol. **35**(6), 1157–1167 (2017).
4. G. Rademacher, R. Luís, B. Puttnam, T. Eriksson, R. Ryf, E. Agrell, R. Maruyama, K. Aikawa, Y. Awaji, H. Furukawa, and N. Wada, "High capacity transmission with few-mode fibers," J. Lightwave Technol. **37**(2), 425–432 (2019).
5. R. Ryf, N. Fontaine, S. Wittek, K. Choutagunta, M. Mazur, H. Chen, J. Alvarado-Zacarias, R. Amezcua-Correa, M. Capuzzo, R. Kopf, A. Tate, H. Safar, C. Bolle, D. Neilson, E. Burrows, K. Kim, M. Marianne Bigot-Astruc, F. Achten, P. Sillard, A. Amezcua-Correa, J. Kahn, and J. J. C. Schröder, "High-spectral-efficiency mode-multiplexed transmission over graded-index multimode fiber," in *European Conference on Optical Communication* (2018), p. h3B.1.
6. T. Sakamoto, K. Saitoh, S. Saitoh, Y. Abe, K. Takenaga, A. Urushibara, M. Wada, T. Matsui, K. Aikawa, and K. Nakajima, "120 spatial channel few-mode multi-core fibre with relative core multiplicity factor exceeding 100," in *2018 European Conference on Optical Communication (ECOC)* (IEEE, 2018), p. We3E.5.
7. G. Rademacher, B. Puttnam, R. Luís, J. Sakaguchi, W. Klaus, T. Eriksson, Y. Awaji, T. Hayashi, T. Nagashima, T. Nakanishi, T. Taru, T. Takahata, T. Kobayashi, H. Furukawa, and N. Wada, "10.66 Peta-Bit/s Transmission over a 38-Core-Three-Mode Fiber," in *Optical Fiber Communication Conference (OFC) 2020* (Optical Society of America, 2020), p. Th3H.1.
8. F. Hamaoka, M. Nakamura, S. Okamoto, K. Minoguchi, T. Sasai, A. Matsushita, E. Yamazaki, and Y. Kisaka, "Ultra-wideband wdm transmission in s-, c-, and l-bands using signal power optimization scheme," J. Lightwave Technol. **37**(8), 1764–1771 (2019).
9. A. Napoli, J. K. Fischer, S. Namiki, M. M. Filer, and V. Curri, "Guest editorial ultra wideband wdm systems," J. Lightwave Technol. **38**(5), 998–1001 (2020).
10. L. Galdino, A. Edwards, W. Yi, E. Sillekens, Y. Wakayama, T. Gerard, W. S. Pelouch, S. Barnes, T. Tsuritani, R. I. Killey, D. Lavery, and P. Bayvel, "Optical fibre capacity optimisation via continuous bandwidth amplification and geometric shaping," IEEE Photonics Technol. Lett. **32**(17), 1021–1024 (2020).
11. B. Puttnam, R. S. Luís, G. Rademacher, L. Galdino, D. Lavery, T. A. Eriksson, Y. Awaji, H. Furukawa, P. Bayvel, and N. Wada, "0.61 Pb/s S, C, and L-Band Transmission in a 125μm Diameter 4-core Fiber Using a Single Wide-band Comb Source," Journal of Lightwave Technology (to be published) DOI: 10.1109/JLT.2020.2990987.
12. https://www.fiberlabs.com/bt_amp_index/s-band-bt-amp/, Accessed on 08/18/2020.
13. S. Gross, N. Riesen, J.-D. Love, and M. Withford, "Three-dimensional ultra-broadband integrated tapered mode multiplexers," Laser Photonics Rev. **8**(5), L81–L85 (2014).
14. R. Maruyama, N. Kuwaki, S. Matsuo, and M. Ohashi, "Two mode optical fibers with low and flattened differential modal delay suitable for wdm-mimo combined system," Opt. Express **22**(12), 14311–14321 (2014).
15. T. Pfau, S. Hoffmann, and R. Noé, "Hardware-efficient coherent digital receiver concept with feedforward carrier recovery for *m*-qam constellations," J. Lightwave Technol. **27**(8), 989–999 (2009).
16. G. Rademacher, R. S. Luís, B. J. Puttnam, H. Furukawa, Y. Awaji, R. Maruyama, K. Aikawa, and N. Wada, "Investigation of higher order modulation formats for few-mode fiber sdm transmission systems," in *2018 IEEE Photonics Society Summer Topical Meeting Series (SUM)* (IEEE, 2018), pp. 147–148.
17. G. Rademacher, R. Ryf, N. Fontaine, H. Chen, R.-J. Essiambre, B. Puttnam, R. Luís, Y. Awaji, N. Wada, S. Gross, N. Riesen, M. Withford, Y. Sun, and R. Lingle, "Long-haul transmission over few-mode fibers with space-division multiplexing," J. Lightwave Technol. **36**(6), 1382–1388 (2018).